XXIV Biennial Symposium on Measuring Techniques in Turbomachinery
Prague, Czech Republic, 29 - 31 August 2018
Paper No MTT2418B33

DEVELOPMENT OF LASER LIFETIME PRESSURE SENSITIVE PAINT (PSP) TECHNIQUE FOR UNSTEADY MEASUREMENTS

N. Aye-Addo, N. Long, G. Paniagua, J. Saavedra
Purdue University
USA

Keywords: laser lifetime pressure sensitive paint, unsteady flow, turbine

ABSTRACT

This paper describes the development of the laser lifetime PSP measurement techniques suitable for turbine unsteady flow investigation. The PSP formulation used for this analysis is tris(2,2'-bipyridyl) ruthenium 'Ru(bpy)' adsorbed on a porous Thin Layer Chromatograph (TLC) Aluminum Oxide plastic binder. Two calibration methods (apriori and in-situ) are used with a quasi-continuous burst-mode laser system. The PSP lifetime decay (< 5μs) of each pixel is measured with both Hyper Vision HPV-X2 Shimadzu and Photron FASTCAM SAZ cameras. The in-situ wind tunnel calibration is applied to a wall mounted hump test case which imposes a pressure gradient representative of the aft portion of low pressure airfoil suction side.

INTRODUCTION

Pressure Sensitive Paint (PSP) is a luminescent coating, that provides a global surface pressure distribution based on the monitoring of the quenching mechanisms of luminescence in time [2]. The luminescent molecules (luminophores) are oxygen-sensitive particles that can be dissolved and applied to an oxygen-permeable binder. The technique utilizes the oxygen sensitivity of the paint's fluorescence and phosphorescence after the excitation with an external light source (LED, flash lamp, laser, etc.). Because each molecule behaves effectively as a pressure sensor, PSP techniques offer significantly higher spatial resolution compared to any sensor based pressure measurements.

There are two types of PSP measurements (intensity and lifetime). Intensity PSP measurements require a continuous illumination source and a wind-off image at no-flow conditions. The radiation intensity is recorded with photo multiplier tubes (PMT) or digital cameras (CCD, CMOS). Lifetime PSP requires a pulsed illumination source and does not require a wind-off image. The lifetime decay following a pulsed illumination can also be recorded with PMT's or digital cameras. The principle setup is shown in Figure 1a. The first application of intensity based technique to aerodynamic flows was proposed by Peterson & Fitzgerald in 1980 [1]. A thorough explanation about the technique and its applications can be found in Liu & Sullivan [2].

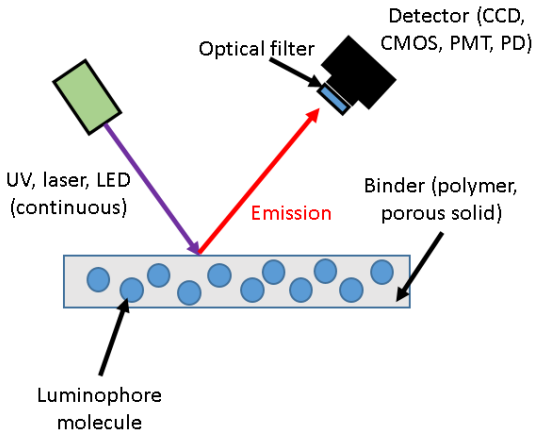

Figure 1: Schematic of a luminescent paint (PSP) on a surface. [2]

The physical process that takes place in a pressure sensitive paint molecule can be explained in detail with the Jablonski energy-level diagram by Bell et. al [3]. A photon of radiation is absorbed to excite the luminophore from its ground electronic state to excited electronic states. The excited electron returns to unexcited ground state by a combination of radiative and radiationless processes. The radiation transition from the lowest excited singlet state to the ground state is called fluorescence. Phosphorescence is the radiative transition from the triplet state to the ground state. In both cases, emission is at a larger wavelength than the excitation.

The radiationless return to ground state is called quenching. Oxygen quenching is the primary photophysical mechanism for PSP. It involves the collision of an excited luminophore with an oxygen molecule leading to an energy transfer and dissipation. The dye molecule returns to the ground state without emitting a photon. The higher presence of oxygen, produces a higher probability of collisions with the luminophore and hence lower the quantum yield Ø.

$$\emptyset = \frac{rate\ of\ luminescence}{rate\ of\ excitation}$$

According to Henry's law, oxygen concentration in the binder is proportional to its partial pressure in ambient air which in turn is proportional to the local static pressure. Both the luminescence intensity or lifetime and pressure can be correlated using the Stern-Volmer equation:

$$\frac{I(P_{ref}, T_{ref})}{I(P,T)} = \frac{\tau(P_{ref}, T_{ref})}{\tau(P,T)} = A(T) + B(T)\frac{P}{P_{ref}}$$

The Stern-Volmer coefficients A and B can be obtained from a paint calibration. Due to thermal quenching (decreasing luminescence intensities at elevated temperatures) they are temperature dependent for most paints. The reference condition for normalized intensity is usually recorded at ambient conditions. This reference is required to compensate for possible sources of error such as paint thickness, or illumination intensity. It has to be acquired before each test and is referred to as "wind-off" image.

Lifetime measurements are acquired with a pulsed illumination and gated camera that requires two subsequent images. Each image is an integration of intensity over gate time. If both images are acquired during luminescence decay that is assumed to be exponential, lifetime can be computed from the intensity ratio. A single or multi-exponential function can be used to fit the luminescent lifetime of the paint after an exciting pulse light ceases. The major advantage of the lifetime technique is compensation of illumination, paint thickness, and model movement errors.

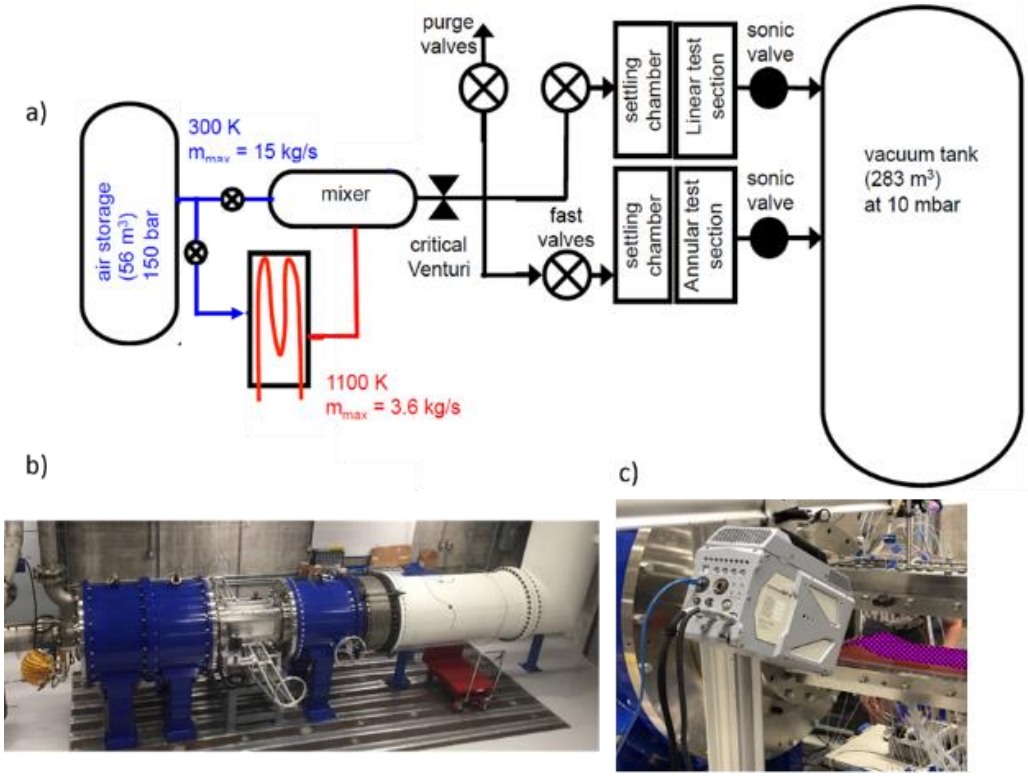

Figure 2: a) Wind tunnel facility, b) Linear wind tunnel, c) Lifetime PSP test set-up

Several researchers have utilized lifetime PSP for aerodynamic applications. Schreivogel et al [4]. applied both the lifetime and intensity method in combination with a temperature-compensated binary paint. Two CCD cameras and pulsed LEDs were used to explore these techniques. Contrary to the intensity method, the lifetime technique was less sensitive to temperature and paint thickness. Yorita et. Al [5] compared LED ('modulation approach") lifetime approach to LASER ("single-shot approach") lifetime PSP techniques. The LED based system used a camera with on-chip accumulation. On the other hand, the LASER based system used a camera with double-shutter mode. The authors found a comparable signal to noise ratio (SNR) for the LASER based lifetime measurement system in comparison to the LED based system, when 128 single images were averaged. A measurement error of 200 Pa was found for the LED based system, whereas 250 Pa was found for the LASER based lifetime system. Unsteady flow phenomenon was captured with the LASER based system.

METHODOLOGY

Experimental Facility

The Purdue Experimental Turbine Aero-Thermal Laboratory linear blow down wind tunnel was used for the in-situ calibration and experimental investigation [6]. The facility layout is depicted in Figure 2a, upstream of the test section compressed dry air at 150 bar is stored in a 56 cubic meter pressure reservoir. Two different lines divert from the high pressure tanks, the first one guides the flow right into the test cell and discharges the flow in a mixer. The second line diverts the air through the heat exchanger where natural gas is burn. The passage of the flow through the heat exchanger provides non-vitiated flow at higher total temperatures. The heated supply is then diluted with cold line in the mixer.
The mass flow ratio between both lines determines the operational flow temperature of the experiment. Several elbows are placed in the pipeline downstream of the mixer to enhance the blending between both fluids and guarantee uniform flow temperature. The air is then discharged through a calibrated critical Venturi that provides accurate mass flow measurements.

While the heat exchanger is being heated up and stable operational conditions are achieved, the air is vented through a purge line. Once the facility runs at steady conditions the purge valve is closed and the valve upstream of the wind tunnel is suddenly opened to discharge the flow through the linear wind tunnel as shown in Figure 2b. the sudden release air is radially discharged inside of the settling chamber, which slows down and straightens the flow as it goes through several honeycombs and screens. The flow is then accelerated through a circular to rectangular contraction area and finally discharged to the linear test section with uniformly spatial and temporal flow conditions. Ultimately, the flow is released to the vacuum tank through a sonic valve. The sonic valve isolates the test article from the downstream conditions once it is choked and provides the independent settlement of Reynolds and Mach numbers.

The test article for the lifetime PSP experiment is a wall mounted hump, depicted in Figure 2c [7]. The wall mounted hump replicates the pressure distribution across a low pressure turbine passage, where flow diffusion takes place downstream of the blade throat. The boundary layer may detach through the pressure gradient and generate a recirculated flow region. The hump was particularly designed to generate a 15 cm recirculated flow region when operating at low Reynolds environments, Re/m of 4 x 10^5 and no separation at all when operating at higher Reynolds, Re/m 6 x 10^6. At the low Reynolds operation, the flow momentum inside of the boundary layer is insufficient to overcome the adverse pressure gradient and the boundary layer detaches from the wall slightly downstream of the hump summit.

Paint and binder formulation

The ingredients for Ru(bpy)-TLC are 6 mg of Ru(bpy) dissolved in 25 ml of Ethyl Alcohol. The solution is stirred until fully dissolved. The ratio of paint molecules to solvent was selected based on similar PSP recipes in Liu & Sullivan [2]. A porous Aluminum oxide thin-layer chromatography plate was used as a binder. Although this option for a binder is fragile for complex geometries, a short response time of the PSP can be obtained using this porous material on a simple geometry. After the paint molecules are dissolved in the solvent, the binder is dipped into the solution to soak overnight. Before testing, the PSP test coupon is carefully removed from the solution and air dried for about 20 minutes. Following, an epoxy adhesive is used to attach the PSP coupon to the test article. During this process the PSP coupon is gently attached to avoid chipping of the binder. The absorption and emission spectra of Ru(bpy) is shown in Figure 4. With a silica TLC binder, Ru(bpy) has a lifetime at room temperature of 3 μs [2].

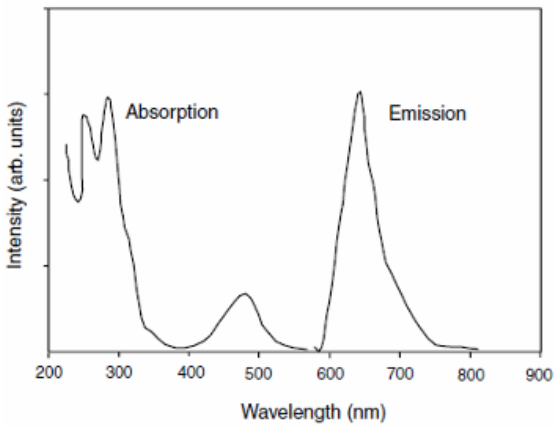

Figure 4: Absorption and emission spectra of Ru(bpy) [2]

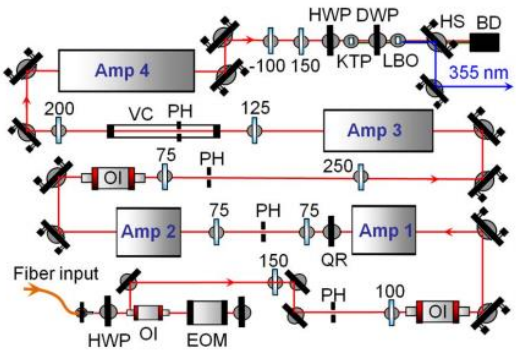

Figure 5: Optical layout of laser system (numbers are focal lengths of spherical lenses) [8]

Illumination source and digital imaging

A state-of-the-art quasi-continuous burst-mode Nd: YAG laser manufactured by Slipchenko et al. [8] was utilized to excite the paint at a 532 nm (2nd harmonic output of the laser). The pulse-burst duration of the laser is 10 milli-seconds with repetition rates of 10 kHz and 20 kHz. The laser has a linewidth of < 2 GHz at 1064.3 nm with 150 mJ per individual pulse at 10 kHz. Compared to previous flash lamp-pumped designs the pulse-burst duration is extended by one order of magnitude due to addition of a fiber oscillator and diode pumped solid state amplifiers. An optical layout of the quasi-continuous burst-mode laser system is shown in Figure 5.

Two different digital cameras were used for the a-priori calibration of the PSP test coupon in a calibration chamber and the in-situ calibration and testing of the PSP coupon on the wall mounted hump test section in the wind tunnel. A Hyper Vision HPV-X2 Shimadzu camera with a maximum sampling rate of 10 MHz (50,000 pixels) was used for the a-priori calibration setup. A 532 nm notch filter and a 610 nm long pass optical filter were used to damp out the incident green laser wavelength and only collect the emission spectra of the PSP. The Shimadzu also has a setting that saves 16-bit TIFF images. A Photron FASTCAM SAZ camera with a maximum sampling rate of 2 MHz (128 x 8 pixels) was used for the in-situ calibration and wind tunnel testing with the wall mounted hump. Similarly, a 532 notch filter and 628 nm (± 16) band pass filter was used to discard the incident laser green light and only collect the PSP emission spectra. The comparison for both cameras is shown in Table 1.

Table 1: Settings for Photorn SAZ and Shimadzu HPV-X2

	FPS	Shutter	Resolution
Shimadzu	5 MHz	110 ns	400 x 250
Photron SAZ	1 MHz	1 µs	40 x 128

A-priori calibration setup

A simple calibration chamber was designed to test the luminescent lifetime decay of a 1" x 1" PSP test coupon. The chamber was spray coated with black matte paint to minimize reflections of the illumination source and ambient lights. A fused quartz window was attached to the chamber to provide optical access for the laser and camera. A GE DPI 610 pressure calibrator was connected to the chamber to provide a range of vacuum and positive pressures over the PSP test coupon. The calibration setup is shown in Figure 6. A combination of both a Plano-convex lens and divergent lens is required to refocus the light. An oscilloscope was used to assess the timing parameters of the laser and camera before calibration data were acquired. The test configuration for a-priori calibration is provided in Table 2.

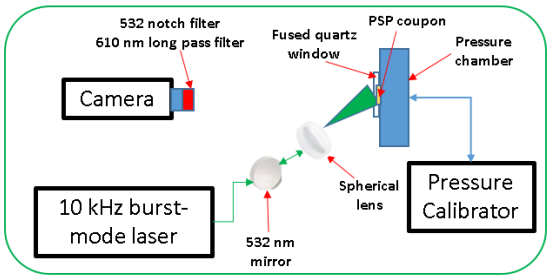

Figure 6: A-priori calibration setup (camera, pressure calibrator, calibration chamber, optical filters and lenses, diffuser, PSP test coupon

Table 2: A-priori calibration test setup parameters

Calibration points	6.2, 8.7, 12.7, 14.6, 16.7, 18.7, 20.7, 22.66 [psia]
Laser	10 kHz bursts (10.5 ms burst width) every 10 seconds
	Singlet pulse train (532 nm wavelength)
	Internal triggering
Camera (Shimadzu)	5 MHz acquisition rate (400 x 250) - 128 frames
	Exposure time: 110 ns
	External standby triggering

The timing signals for the experiment were driven by TTL pulses from the Quantum Composer 9530 series pulse generator. The camera was configured to capture an image series which contained a dark reference (to account for background camera noise), high intensity image (immediately after laser pulse), and luminescent lifetime decay images. To capture these images, the camera must be triggered immediately before a laser pulse. Since the laser cannot achieve full power on first pulse, the camera trigger was set to occur near middle of pulse train at t + 5ms. It was then pushed forward to by five frames (1µs) to capture multiple dark background images. Finally, a 10 ns offset was added to delay the camera and account for the nominal width of the laser pulse. Ideally, this 10 ns addition kept the laser pulse out of all exposures since it occurred in the final 10 ns of the 90 ns (dead time) between the last dark exposure and initial intensity image. The pulse generator jitter is negligible at 250 ps. Therefore, the laser was triggered at $t_0 = 0$ and the camera was triggered at
$t = t_0 + 4.999010$ ms. A summary of the timing configuration for the apriori calibration setup is shown in Figure 7.

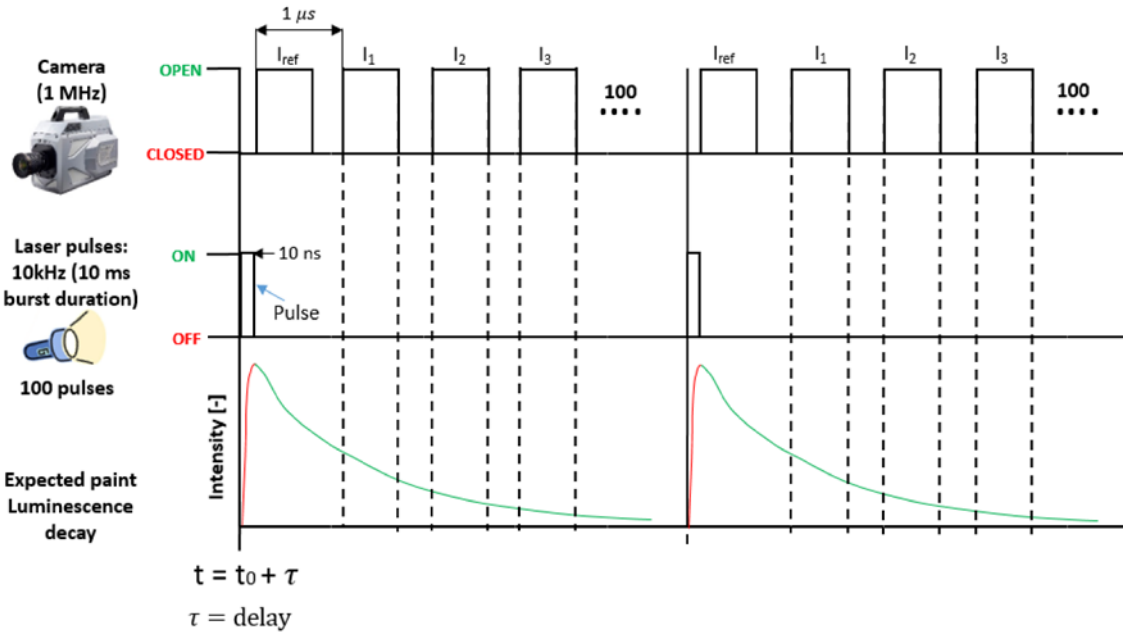

Figure 7: Laser and camera timing configuration for a-priori calibration

In-situ calibration setup

An in-situ calibration with the similar PSP setup Ru(bpy)-TLC was applied to the wall hump test section. The test setup is shown in Figure 8. The same laser system was used to illuminate the paint and due to availability a Photron SAZ fastcam was used for calibration and acquiring data during wind tunnel runs instead of the Shimadzu. A camera calibration procedure using a direct linear transformation method by Liu et. al [9,10] was utilized to map points in the raw image space to the physical model space. This technique was recently implemented by Husen et al. [11].

For camera calibration, a dot target is positioned on the test article in the wind tunnel at different heights with known model space dimensions. In this case, the dots had a diameter of 0.25" and were spaced 1" in both vertical and horizontal directions. The full resolution of the camera was used during the camera calibration (1024 x 1024 pixels) and the pixel size was (20 x 20 micro-meters). The first step in the camera calibration process is to determine both the horizontal and pixel spacing in the calibration photos. An example of the dot target placed on the test article is shown in Figure 9a.

The thickness of the dot target is 0.25". Based on the resolution of the calibration photos, 4 dots were used in a row and 5 rows were selected in a plane. Three height levels at 0.25", 0.5" and 0.75" were selected to capture the mapping of the image to the model space. Next, any rotation or translational shifts needed for coordinate system is applied. After these steps, the centroids of the dots are used in the calibration technique to build up the image space. A direct linear transformation is applied in order to directly map the image space to the object or model space. Finally, a grid is generated mapping the entire image surface in 3D, which is shown in Figure 9b.

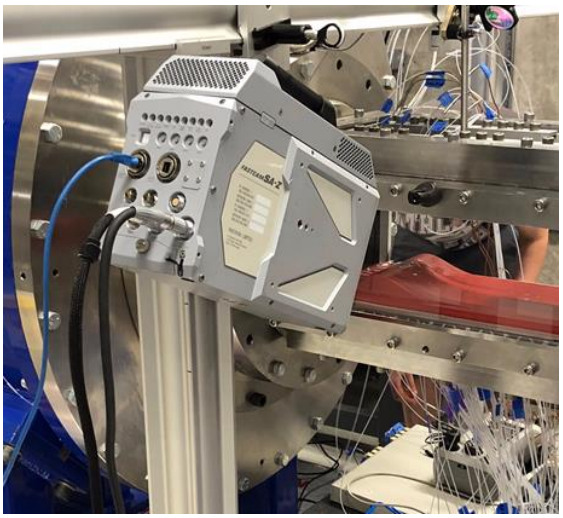

Figure 8 In-situ PSP calibration test setup

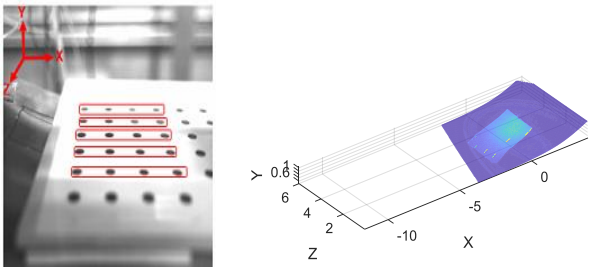

Figure 9: a) Dot target b) Mapping of image surface in 3D

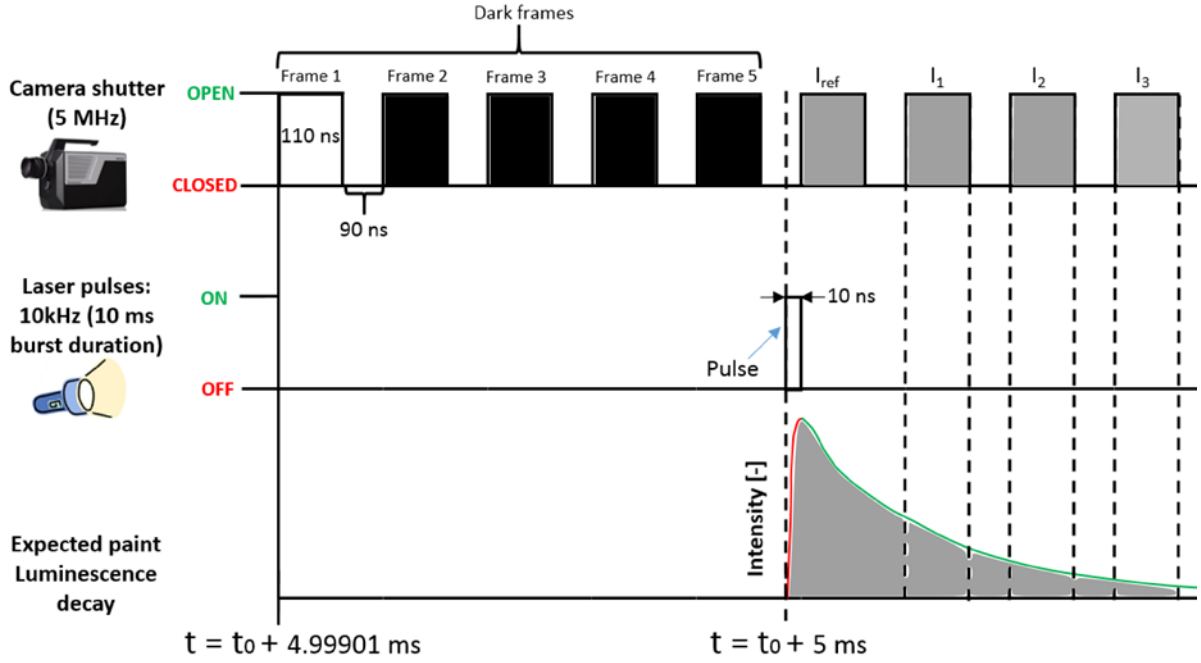

Figure 10: Laser and camera timing configuration for in-situ calibration

During a calibration test, the laser beam is guided through a set of mirrors and lenses on an optical rail and finally enters through an optical window on the top of the test section to illuminate the PSP test coupon. The camera is mounted a beam extending from the optical rail and is angled to acquire images from the lateral optical window. The Photron SAZ camera was sampled at 1 MHz and laser was run at 10kHz burst mode for a duration of 10 ms. This combination allowed multiple data sets in order to compare repeatability of the experiments as compared to the a-priori calibration setup where only one laser pulse data point was used. The summary of experiments is shown in Table 3. The laser and camera timing is also shown in Figure 10. The camera was triggered to acquire data after a delay of 300 ns from the laser pulse to avoid over exposing or saturating the sensor with the laser beam.

Table 3: In-situ calibration test setup parameters

Calibration points	11.5, 11.95, 12.3, 12.7, 13.05, 13.37, 13.55, 13.9, 14.2, 14.7 [psia]
Laser	10 kHz (10.5 ms burst width) every 10 seconds
	Singlet pulse train (532 nm wavelength)
	Internal triggering
Camera (Photron SAZ)	1 MHz acquisition rate (128 X 40)
	External triggering

RESULTS AND DISCUSSION

A-priori lifetime calibration results

An example of a photo acquired during luminescence decay is shown Figure 11. The non-uniformity of the laser illumination could be an effect of diffuser and Plano convex lens not placed correctly so that the laser beam spreads out too much. Additionally, the dipping process of the TLC binder in the (paint + solvent) formulation could also have some non-uniform effects as well. The pixel-by-pixel time constants results at 6.2 psi is shown in Figure 12. The time constant calculation required at least 3 images after the laser pulse to fit an exponential decay curve. Any pixel that failed to meet this criterion was removed. This could be attributed to the non-uniformity in illumination of the PSP coupon.

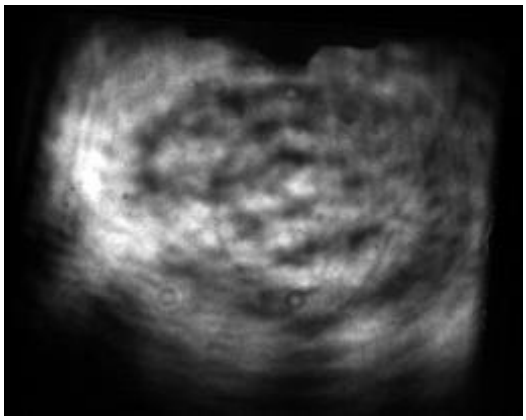

Figure 11: Acquired image during PSP luminescence decay

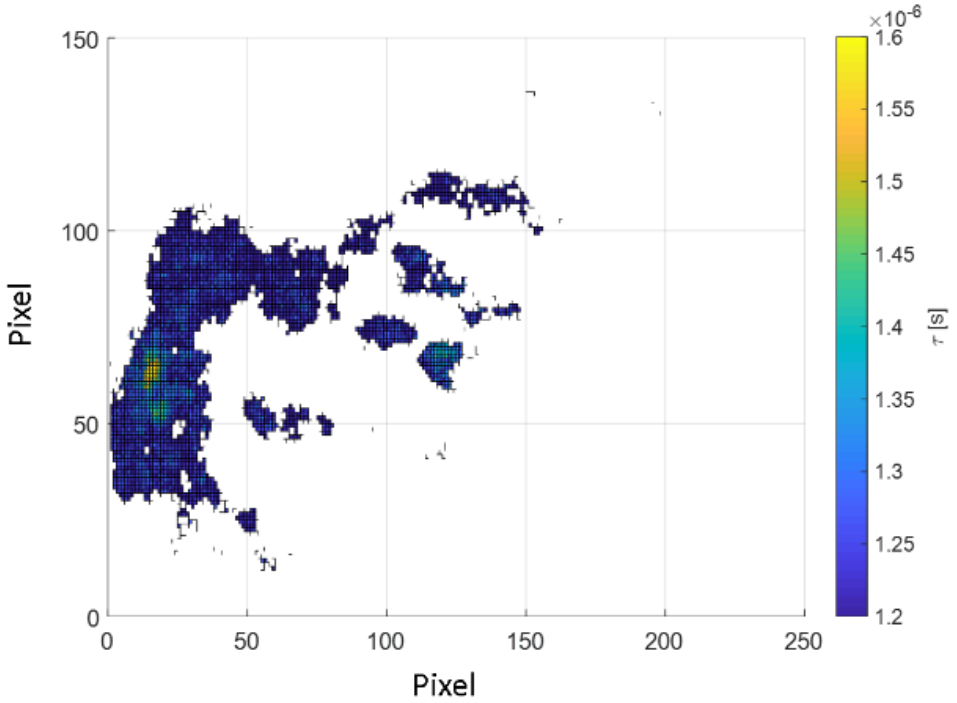

Figure 12: Pixel by pixel decay time constant (6.2 psi)

The variation between each pixel can be seen in Figures 13 and 14. Figure 13 shows a specific pixel where 7 images were used to calculate the lifetime decay and Figure 14 shows a specific pixel where only 3 images were used. As a rule, more than 2 data points (images) are needed to generate a good lifetime decay fit. A single exponential term was used to fit the lifetime decay data and a rule of 5τ was applied to calculate the exponential time constant. This implies that the intensity has reduced to less than 1% of its original value, therefore almost decayed to zero. Figure 15 shows an example of an exponential fit with the discrete points for each image used in lifetime decay calculation at a specific pixel. The range of lifetime values fall between 1.2 and 1.7 µs which is less compared to the literature at ambient pressure and temperature (3-5 µs).

For each pressure calibration point, the mean time constant was also calculated. Figure 16 shows the time constants plotted against each pressure calibration point. The correlation between time constant and pressure was inverse to what was expected. Additionally, Figure 17 shows the spatially averaged luminescent decay at each pressure. Both plots show there is a weak relationship between increasing pressure and decreasing lifetime decay. Therefore, these calibration results were not applied to the surface pressure measurements on the wall-mounted hump test section in the linear wind tunnel.

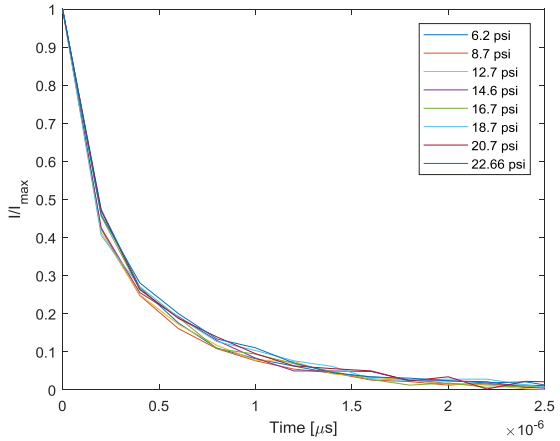

Figure 13: Lifetime decay at specific pixel (j = 63, k = 15) with 7 images

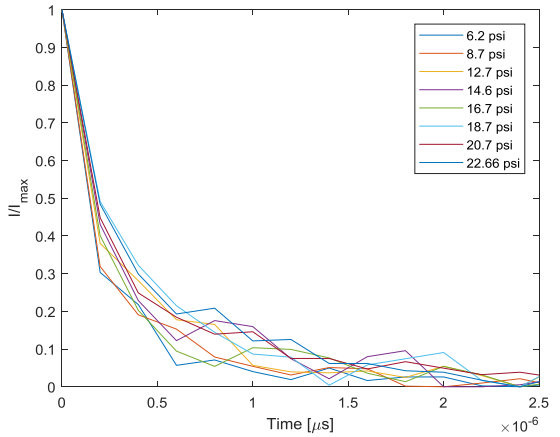

Figure 14: Lifetime decay at specific pixel (j = 22, k = 102) with 3 images

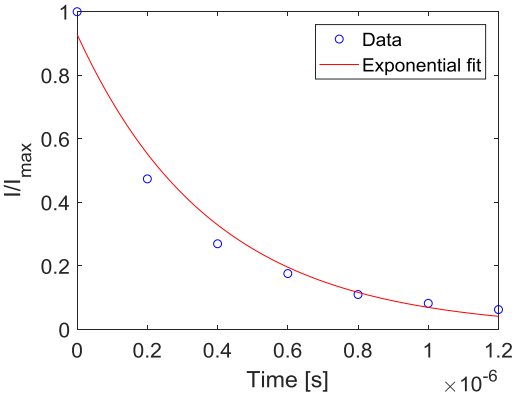

Figure 15: Exponential decay fit at single pixel (6.22 psi)

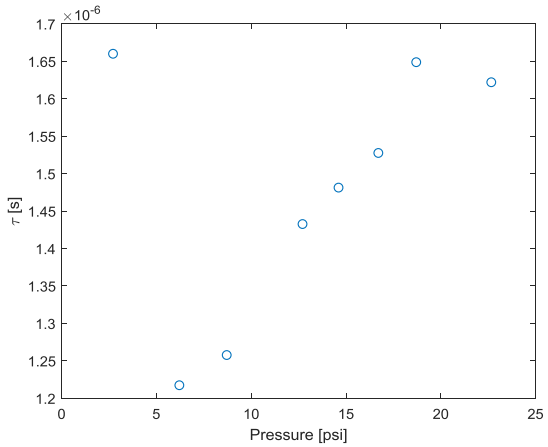

Figure 16: Time constant at each pressure calibration point

In-situ lifetime calibration results

The pixel-by-pixel variation in the time constant is shown in Figure 18 at pressure calibration point of 11.5 psi. Compared to the a-priori results, these

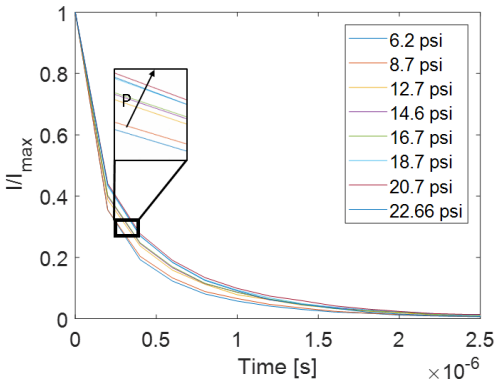

Figure 17: Spatially averaged lifetime decay for all pressure calibration points

values are more spatially uniform. However, it should also be noted that the resolution is much smaller in this case compared to the a-priori results. The exponential fit to the lifetime decay at a specific pixel (j=20, k=60) is shown in Figure 19. This pixel was selected since it has a high R^2 value for the correlation fit. In Figure 20, the spatially averaged lifetime decay at all the pressure calibration points is also shown. The pressure calibration points and decay time constant follows the correct trend with increasing pressure. The variation in time constant is very small compared to the change in pressure. The spatially averaged decay time constant for each pressure calibration is computed and a second order polynomial is used to find a calibration curve for computing pressure. This is shown in Figure 21. A 2nd order polynomial calibration curve produced a lower R^2 value of ~ 0.96.

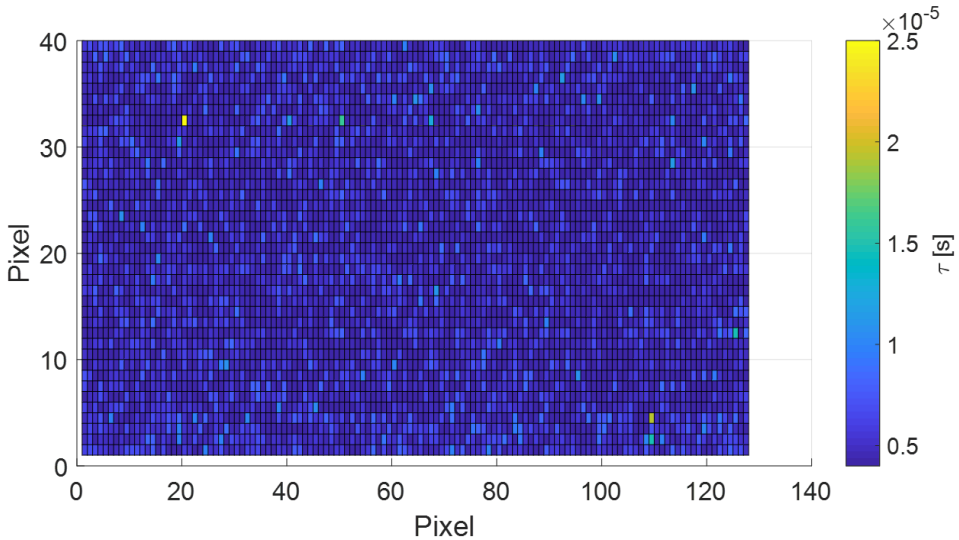

Figure 18 Pixel by pixel decay time constant (11.5 psi)

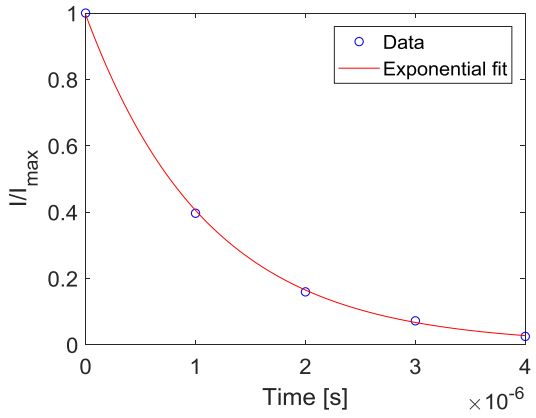

Figure 19: Exponential decay fit at single pixel (11.5 psi)

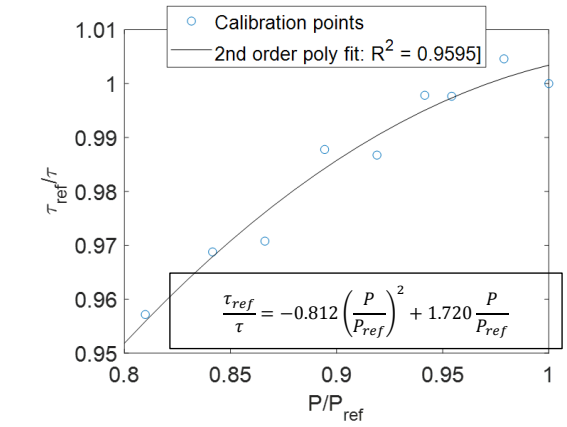

calibration curve for Ru(bpy)-TLC

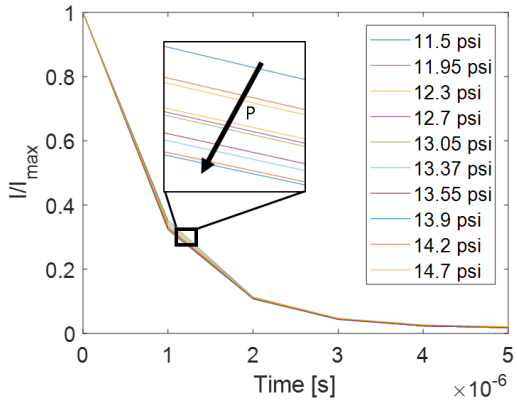

Figure 20: Spatially averaged lifetime decay for all pressure calibration points

CONCLUSIONS

This paper discusses a laser lifetime measurement technique suitable for unsteady flows. The technique is developed as proof-of-concept with an a-priori calibration and supported with an in-situ calibration setup in a blow down linear wind tunnel. Several iterations were attempted to configure both calibration setups include PSP formulation, laser and camera setup. The pixel-by-pixel calibration results are compared between a-priori and in-situ calibrations. The in-situ calibration is performed in the Purdue Experimental Turbine AeroThermal Lab. A calibration curve is applied to the data for future post-processing.

ACKNOWLEDGEMENTS

The authors want to thank Prof. John Sullivan for providing the PSP paint molecule and binder, Jordan Fisher for setup of laser during in-situ calibration and templates for post-processing code, Terry Meyer and Mikhail Slipchenko for providing the laser, and Nick Husen for providing a template for camera calibration photogrammetry toolbox. Finally, we want to acknowledge the financial support of Rolls-Royce corporation.

REFERENCES

[1] Peterson, J. I. and Fitzgerald, R. V.; 1980. “New technique of surface flow visualization based on oxygen quenching of fluorescence”. Review of Scientific Instruments, 51(5):670{671.

[2] Liu, T. and Sullivan J. P.; 2005. “Pressure and Temperature Sensitive Paints”. Springer.

[3] Bell, J.H.; Schairer, E.T.; Hand, L. A. et al.; 2001. “Surface Pressure Measurements Using Luminescent Coatings”. Annual Review of Fluid Mechanics, 33:155{206,.

[4] Schreivogel, P.; Paniagua, G.; Bottini, H.; 2012. “Pressure Sensitive Paint Techniques for Surface Pressure Measurements in Supersonic Flows”. Experimental Thermal and Fluid Science, 39:189-197, DOI: 10.1016/j.expthermflusci.2012.01.023

[5] Yorita, D.; Weiss, A.; Geisler, R. et al.; 2018. “Comparison of LED and LASER based Lifetime Pressure-Sensitive Paint Measurement Techniques”. AIAA SciTech 2018, 8-12 Jan 2018, Kissimmee, Florida, DOI: 10.2514/6.2018-1029

[6] Paniagua G.; Gonzalez Cuadrado D.; Saavedra J.; Andreoli V.; Meyer T.; Solano J. P.; Herrero R.; Meyer S.; Lawrence D.; 2018. “Design of the Purdue Experimental Turbine Aerothermal Laboratory for optical and surface aero-thermal measurements”. Journal of Engineering for Gas Turbines and Power. DOI: 10.1115/1.4040683. ISSN: 0742-4795.

[7] Saavedra, J.; Paniagua, G.. “Transient Performance of Separated Flows: Characterization and Active Flow Control “. Journal of Engineering for Gas Turbines and Power. doi:10.1115/1.4040685

[8] Slipchenko, M. N.; Miller, J. D.; Roy, S.; Gord, J. R.; Danczyk, S. A. and Meyer, T. R.; 2012. “Quasi-Continuous Burst-Mode Laser for High-Speed Planar Imaging”, Optics Letters, 37(8), 1346-1348

[9] C. Y. Huang, C. M. Lai and J. S. Li, 2012. "Applications of Pixel-by-Pixel Calibration Method in Microscale Measurements with Pressure-Sensitive Paint," in Journal of Microelectromechanical Systems, vol. 21, no. 5, pp. 1090-1097, Oct. 2012. doi: 10.1109/JMEMS.2012.2203106

[10] Liu, T. and Burner, A. W.; 2014. “Photogrammetry toolbox reference manual”.

[11] Liu, T.; Cattafesta, L.; Radeztsky, R. and Burner, A.; 2000. “Photogrammetry applied to wind-tunnel testing,” AIAA Journal, Vol. 38, No. 6, pp. 964–971 doi: 10.2514/2.1079

[12] Husen, N.; Sullivan, J. P.; Liu T.; 2017. “The Luminescent Oil-Film Flow-Tagging (LOFFT) Skin-Friction Meter Applied to FAITH Hill”, AIAA Scitech Forum January 2017, Grapevine, Texas, 55th AIAA Aerospace Sciences Meeting,